THE JOURNAL OF PHYSICAL CHEMISTRY C

Article

pubs.acs.org/JPCC

Hydrogenation Study of NaF/NaH/MgB_2 Reactive Hydride Composites

J. L. Carrillo-Bucio,[†] I. Saldan,[‡,§] C. Pistidda,[‡] F. Karimi,[‡] K. Suárez-Alcántara,[*,†,‡] M. Dornheim,[‡] and T. Klassen[‡]

[†]Unidad Morelia del Instituto de Investigaciones en Materiales, Universidad Nacional Autónoma de México, Antigua Carretera a Pátzcuaro No. 8701, Col. Ex Hacienda de San José de la Huerta, C.P. 58190, Morelia, Michoacán, Mexico

[‡]Materials Technology, Institute of Materials Research, Helmholtz-Zentrum Geesthacht, D-21502 Geesthacht, Germany

Supporting Information

ABSTRACT: The hydrogenation of NaF/9NaH + $5MgB_2$ and NaF/2NaH + $1.5MgB_2$ reactive hydride composites (RHC) was studied by volumetric titration (kinetics and PCI curves), in situ synchrotron radiation powder X-ray diffraction (SR-PXD), high-pressure differential scanning calorimetry (HP-DSC), Fourier transform infrared spectroscopy (FT-IR), and scanning electron microscope (SEM). A hydrogen uptake between 4.1 and 4.8 wt % was observed when the H_2 pressure was in the range between 25 and 50 bar, and the temperature was kept constant at 325 °C. PCI curves indicate a hydrogenation equilibrium pressure of 2 and 8 bar at 325 °C for NaF/9NaH + $5MgB_2$ and NaF/2NaH + $1.5MgB_2$, respectively. Synchrotron radiation powder X-ray diffraction revealed the formation of solid solutions of NaF−NaH after milling and a change in the reaction pathway compared to a reported nondoped 2NaH + MgB_2 reactive hydride composite. Formation of the stable side-product $NaMgH_2F$ was found as a drawback for hydrogen storage capacity and reversibility. FT-IR indicates no hydrogen to fluorine substitution in the $NaBH_4$ product.

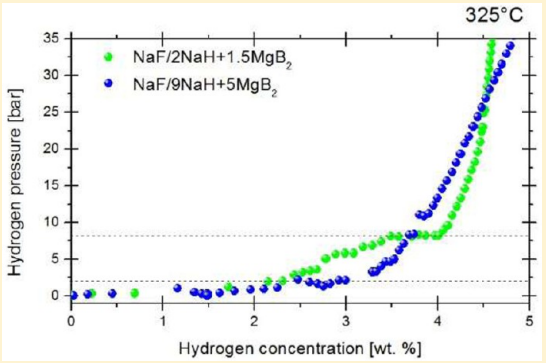

1. INTRODUCTION

Efficient hydrogen storage is a key factor for the development and commercialization of fuel cell applications. Hydrogen storage in solid-state materials has been proposed as the ideal storage method for demanding applications. Despite the lack of the "ideal" hydrogen storage material, the alanates and borohydrides arise as possible contenders. Light-metal borohydrides have a high hydrogen storage capacity; however, their rehydrogenation has been proved to be difficult.[1] Clever mixing of metal borohydrides and metal hydrides had produced promising materials due to the possibility of lowering the dehydrogenation enthalpy, improving kinetics or reversibility.[2,3] These systems had been identified as reactive hydride composites (RHCs). A well-studied and promising system of the RHC concept is the $2LiBH_4 + MgH_2 \leftrightarrow 2LiH + MgB_2 + 4H_2$.[4] However, other interesting systems with the same reaction scheme, such as the $Ca(BH_4)_2$−MgH_2 [5] and the $NaBH_4$−MgH_2 [6] RHCs, had been studied too.

Careful studies on the system

$$2NaBH_4 + MgH_2 \leftrightarrow 2NaH + MgB_2 + 4H_2 \quad (1)$$

had proved a decrease of the dehydrogenation temperature of about 40 °C compared to pure $NaBH_4$, and a relative easy formation of $NaBH_4$ when starting from 2NaH + MgB_2.[7,8] Further reduction of the hydrogenation/dehydrogenation temperature and an improvement of reactions kinetics are expected by the use of suitable additives. A wide selection of additives had been tested; the list includes, but it is not limited to, $ZrCl_4$, Zr isopropoxide, VCl_3, V triisopropoxide, $TiCl_3$, $TiCl_4$, Ti isopropanol, various transition-metal oxides such as Nb_2O_5, etc.[9,10] Among them and commonly observed, metal fluorides additives appear reducing dehydrogenation temperature of $NaBH_4$.[11] Changes in the hydrogenation/dehydrogenation reactions pathways had been observed in the $Ca(BH_4)_2 + MgH_2 \leftrightarrow CaH_2 + MgB_2 + 4H_2$ and the $2LiBH_4 + MgH_2 \leftrightarrow 2LiH + MgB_2 + 4H_2$ systems by the use of fluorinated additives of the same structure as the simple hydride of the dehydrogenated state, i.e., CaF_2 or LiF, respectively.[12,13] Mao et al. demonstrated the reversible hydrogenation of 2NaF + MgB_2 catalyzed with TiF_3, to the formation of $NaBH_4$, MgF_2, and $NaMgF_3$.[14] In a recent study, the effect of adding NaF to the RHC 2NaH + MgB_2 was analyzed.[15] In that study, where the addition of NaF accounted for 10 mol % versus the total NaH content, the effect of milling time and the hydrogenation products were analyzed. Here we present a hydrogenation study of a NaH + MgB_2 RHC mixed with NaF in two proportions: NaF/9NaH + $5MgB_2$ (10 mol % of NaF) and NaF/2NaH + $1.5MgB_2$ (33 mol % of NaF). The materials were hydrogenated at two pressures: 25 and 50 bar. The influence of NaF on the hydrogenation of the 2NaH + MgB_2 RHC is

Received: September 28, 2016
Revised: January 9, 2017
Published: January 11, 2017

DOI: 10.1021/acs.jpcc.6b09776
J. Phys. Chem. C 2017, 121, 4093−4102

discussed based on morphology, reaction pathway, kinetics, impurities, and PCI curves.

2. EXPERIMENTAL DETAILS

2.1. Materials Preparation. The reactive hydride composites NaF/9NaH + 5MgB_2 and NaF/2NaH + 1.5MgB_2 were prepared in two sequential ball mill steps.[12] In the first step, the NaF and the NaH reactives were ball-milled during 60 h (40 cycles of 90 min milling and 15 min resting). In the second part of the preparation, MgB_2 was added to the resulting NaF−NaH mixtures and ball-milled for additional 27 h (18 cycles of 90 min milling and 15 min resting). All reactives were from Sigma-Aldrich (NaH 95% purity, NaF 99.99% purity, and MgB_2 ≥99% trace metals basis) and used as received. The ball milling was performed in a SPEX 8000 mill. The ball to powder weight ratio was kept at 10:1 in both steps of ball milling. Three zirconium oxide balls of 1 cm diameter were used. Ball milling was performed in batches of 1 g as necessary for characterization.

2.2. In Situ Synchrotron Radiation Powder X-ray Diffraction (SR-PXD). The hydrogenation reactions on NaF/9NaH + 5MgB_2 and NaF/2NaH + 1.5MgB_2 composites were traced by in situ synchrotron radiation powder X-ray diffraction (SR-PXD). The in situ SR-PXD experiments were performed in the beamline I711, at MAX-lab synchrotron facility (λ = 0.946 08 Å)[16] or in D3 beamline at Hasylab, DESY (λ = 0.500 503 Å). The powder samples were compacted inside sapphire single-crystal tubes (o.d. = 1.09 mm, i.d. = 0.79 mm). In turn, the sapphire tubes were attached to a dedicated X-ray diffraction cell.[17] All these operations were performed in an argon-filled glovebox, where humidity and oxygen were maintained below 10 ppm. After appropriate sample to X-ray beam alignment, fixing of the initial H_2 pressure (25 or 50 bar), and programming of the temperature control, X-ray diffraction patterns were collected. The X-ray exposure time was 15 s per powder X-ray diffraction pattern. Suitable reading and clearance time of the CCD detector were allowed between collection of diffraction patterns. The temperature of the samples in the cell was increased at 5 °C min^{-1} from room temperature to 325 °C and kept isothermal for 1 h. Powder diffraction data reduction was performed with the help of the Fit2D program. PXD peak assignment and analysis were performed with the MAUD software. Crystallographic information for phase identification was taken from the Inorganic Crystal Structure Database (ICSD) or the Crystallographic Open Database (COD).

2.3. Scanning Electron Microscopy. Scanning electron microscopy (SEM) images were taken for the as-milled materials and the hydrogenated materials. Samples were extended in carbon tape, attached to a suitable sample holder, and transferred to the SEM microscope with an argon-filled glovebag. Sample images were taken in a JEOL7600F microscope. The acceleration voltage was between 2 and 10 keV. Backscattered electrons or secondary electrons detectors were used for producing the SEM images. The specific experimental SEM conditions were selected according to the sample characteristics and ease of imaging. Energy-dispersive X-ray spectroscopy (EDS) mappings were performed for contamination or impurities search.

2.4. High Pressure Differential Scanning Calorimetry (HP-DSC). Hydrogenation reactions were also performed in a high-pressure differential scanning calorimetry (Netzsch DSC 204 HP Phoenix) at a constant pressure of 25 or 50 bar. The samples were heated at 5 °C min^{-1} from 30 to 470 °C. The DSC measurements and sample preparation were performed in an argon-filled glovebox.

2.5. Hydrogenation Reactions. *Kinetic curves of hydrogenation.* NaF/9NaH + 5MgB_2 and NaF/2NaH + 1.5MgB_2 materials were hydrogenated in a HERA Hydrogen System Hydro Quebec titration machine or in a PCTPro-2000 instrument. The hydrogenation conditions were 25 or 50 bar hydrogen pressure and 325 °C. The operation mode was the following: a sample of about 300 mg was transferred to the HERA machine or to the PCTPro-2000 instrument without contact with the air. At low temperature, the working hydrogen pressure was fixed to 25 or 50 bar; then the sample was heated to 325 °C at 5 °C/min heating rate. The differential pressure between the sample holder plus a reservoir and a reference, i.e., an empty sample holder plus a reservoir of equal characteristics, was recorded at HERA Machine. The differential pressure between the initial pressure and the instant pressure was recorded each second at the PCTPro-2000 instrument. The differential pressures were translated to hydrogen uptake expressed in weight percent by means of adequate real gas state functions and mass balance.

Pressure−Composition-Isotherm (PCI) Curves of Hydrogenation. The hydrogenation PCI curves were performed in an isorbHP1 equipment (high-pressure gas adsorption for gas storage materials characterization of Quantachrome Instruments). 350 mg of sample was placed in a dedicated sample holder and transferred to the equipment without oxygen or moisture contamination. After suitable equipment calibration for void volume with ultrahigh purity helium, the sample holder was heated to 325 °C under dynamic vacuum. Then, hydrogen was introduced to the system in steps, progressively from 0.1 to 35 bar. The steps were 50, and they were equally dispersed along the experimental pressure range. The equilibrium conditions were the following: not any changes in the registered pressure larger than 0.1 mbar during 250 s, or a maximum time of 180 min per step. That translated approximately in 4 days of testing. After testing, the system was cooled down. Then, the pressure was released and the sample was transferred to the glovebox without air (oxygen or moisture) contact.

2.6. Fourier Transform Infrared Spectroscopy. The studied materials were compacted in KBr pellets. The KBr was from Sigma-Aldrich and dried just before the pellet preparation. An amount of 2.5 mg of the hydrogenated samples was dispersed in 50 mg of dry KBr, mixed, and pressed. Pellet preparation was performed in an argon-filled glovebox. FT-IR data were collected in a Varian 640-IR, FT-IR spectrometer in ATR mode.

3. RESULTS

3.1. NaH−NaF Solid Solutions at As-Milled Materials. NaH and NaF share the same group symmetry, i.e., $Fm\bar{3}m$,[18,19] with only a slight change of the cell size (NaH, ICSD-33670, $a = b = c$ = 4.89 Å and NaF, ICSD-44276, $a = b = c$ = 4.76 Å). Figure 1 presents the first diffractograms of the SR-PXD studies; they correspond to the as-milled materials. The dot-green lines mark the expected NaH peaks, and the dot-pink lines mark the NaF expected peaks. The first noticeable characteristic is the merging of NaH and NaF peaks into a single NaH−NaF peaks set. Rietveld refinement of the diffractograms indicates that the NaH−NaF peaks are due to a cubic $Fm\bar{3}m$ structure with size a = 4.85 Å for the NaF/9NaH and a = 4.79 Å for NaF/2NaH, respectively. Thus, a solid

DOI: 10.1021/acs.jpcc.6b09776
J. Phys. Chem. C 2017, 121, 4093−4102

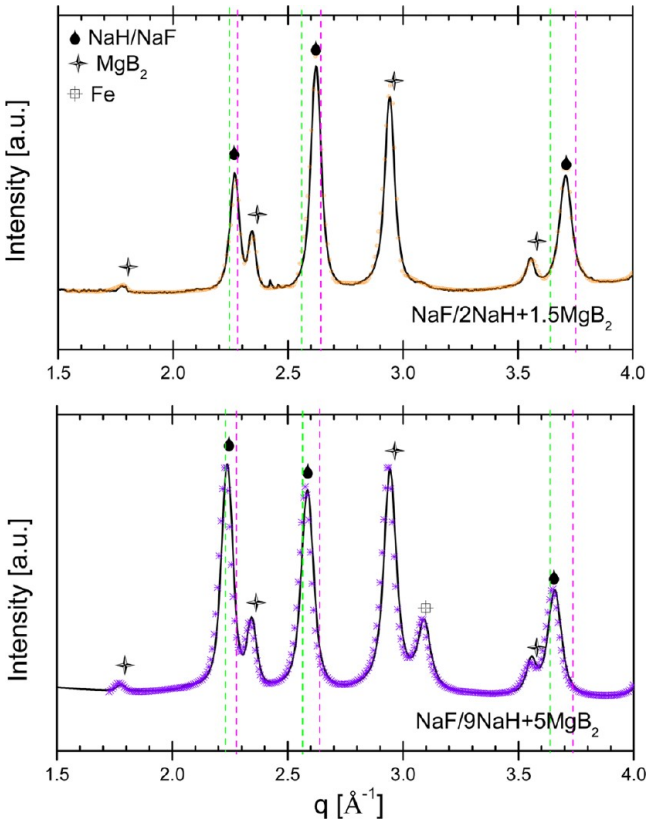

Figure 1. Diffractograms of as-milled materials NaF/2NaH + 1.5MgB_2 and NaF/9NaH + 5MgB_2. Green line indicates expected diffraction peak positions of NaH. Pink line indicates expected diffraction peak positions of NaF.

solution NaH−NaF was formed during ball milling. Another feature was the peak at 3.08 $Å^{-1}$ observed for the NaF/9NaH + 5MgB_2 material. This peak corresponds to Fe (180969-ICSD) contamination from milling vials. Rietveld analysis estimated the amount of Fe as 1.54 ± 0.02 wt % (R_{wp} = 1.934 732 6).

3.2. Scanning Electron Microscopy of As-Milled Materials. Figure 2a presents a high magnification SEM image of as-milled NaF/2NaH. From the Supporting Information images, it can be observed that the NaH/2NaH material formed spherical agglomerates of about 300 μm. A close examination of the agglomerates reveals that they are made of small particles of about 20−35 nm (Figure 2a). In the as-milled NaF/9NaH (Figure 2b and Supporting Information images), the morphology is quite similar to that of the as-milled NaF/2NaH, i.e., agglomerates of about 300 μm composed of smaller particles. However, in this material the small particles were about 40−60 nm. The as-milled NaF/2NaH + 1.5MgB_2 did not present clear agglomerates (Supporting Information). The material was equally dispersed along the SEM-carbon type. In a very ordinary way, this material appearance resembled "boiled oats", without well-defined agglomerate size. Figure 2c present the SEM image of as-milled NaF/2NaH + 1.5MgB_2 at bigger magnifications than in the Supporting Information. Here, particles bellow 1 μm size can be observed. The as-milled NaF/9NaH + 5MgB_2 presented more defined agglomerates of about 300 μm of diameter (Supporting Information). A close inspection of the surface (Figure 2d) reveals that these agglomerates were composed of a mixture of spherical and elongated particles between roughly 1 and 5 μm. EDS results of the as-milled materials reveal that in addition to Na, F, and Mg (B was not registered); Fe, Al, Si, S, Cl, K, Ca, Ti, Ni, Br, Y, Zr, and Ce were found in relatively small quantities. The Fe contribution could come from the milling vial. For the rest of elements, they could come from the milling balls and

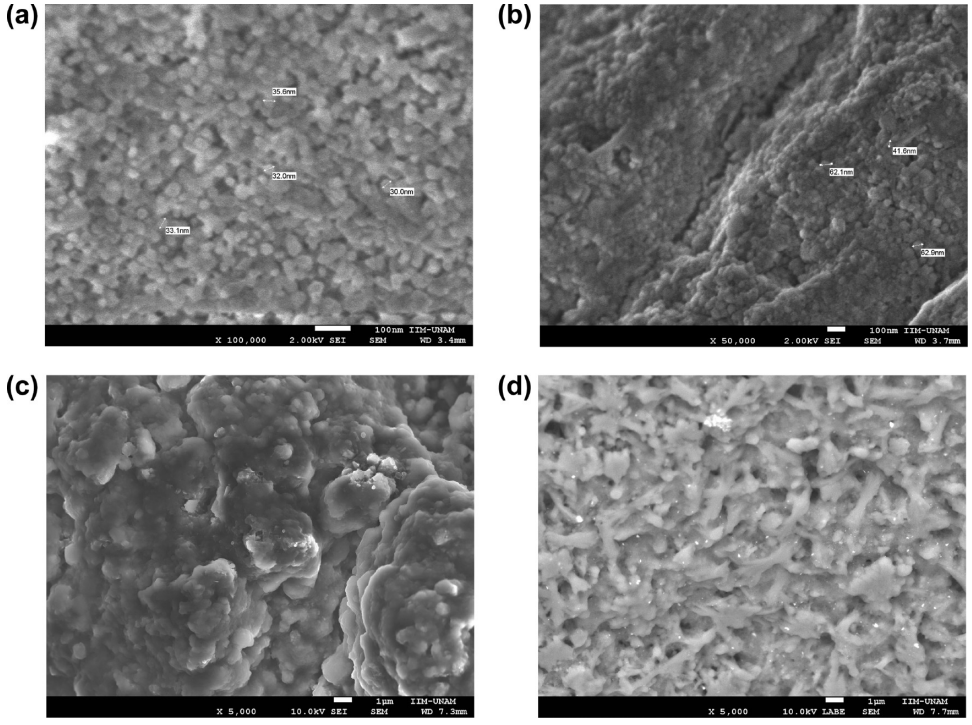

Figure 2. SEM images of (a) as-milled NaF/2NaH, (b) as-milled NaF/9NaH, (c) as-milled NaF/2NaH + 1.5MgB_2, and (d) as-milled NaF/9NaH + 5MgB_2.

DOI: 10.1021/acs.jpcc.6b09776
J. Phys. Chem. C 2017, 121, 4093−4102

principally from impurities of NaH (Sigma-Aldrich NaH 95% purity).

3.3. Hydrogenation by Means of High Pressure Differential Scanning Calorimetry. Figure 3 presents the

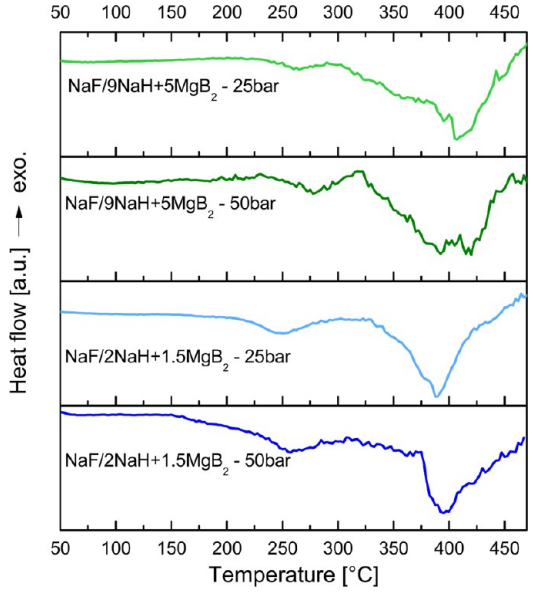

Figure 3. Hydrogenation tracing by means of HP-DSC of both materials NaF/2NaH + 1.5MgB_2 and NaF/9NaH + 5MgB_2 at 25 and 50 bar hydrogen pressure.

hydrogenation tracing by means of HP-DSC of NaF/9NaH + 5MgB_2 and NaF/2NaH + 1.5MgB_2 composites at the two tested pressures, i.e., 25 bar and 50 bar. In all four traces, two broad peaks were observed: one peak with onset temperature roughly above 230 °C and another peak with onset temperature roughly above 300 °C. In situ SR-PXD will help to find out the processes to which these peaks belong and more about the NaF effect.

3.4. In Situ Synchrotron Radiation Powder X-ray Diffraction (SR-PXD). Figure 4 shows the hydrogenation of NaF/9NaH + 5MgB_2 material at 25 bar outlined by in situ SR-XPD. At the front of Figure 4 is presented the as-milled materials at room temperature. The observed peaks correspond to MgB_2, Fe peak at 3.08 $Å^{-1}$ and the presence of a single peak set for the solid solution NaF−NaH. As heating proceeds, at 250 °C, peaks of $NaBH_4$ start to emerge (orange diffractogram). After some time at 325 °C (the isothermal condition), peaks of $NaMgH_2F$ were evident (green diffractogram). After fast cooling no evidence of new crystallized phases appeared (blue diffractogram). The $NaMgH_2F$ [20] shares its perovskite structure with $NaMgH_3$ [19] and $NaMgF_3$:[21] *Pnma* (Supporting Information). All three materials present similar diffraction peaks, though $NaMgH_2F$ (ICSD-91794) agreed better with the observed diffraction peaks. However, it seems that the H and F content in the perovskite structure of the binary hydride can extend in a variety of proportions. Heere et al. founded a partial F content of $NaMgH_{3-x}F_x$, x = 0.848, after hydriding of NaF/9NaH/5MgB_2.[15] The ICSD-91794 file itself records the $NaMgH_2F$ exactly as $NaMg(H_{1.832}F_{1.168})$. Sheppard et al. in a study of the hydriding characteristics of $NaMgH_2F$ proposed the progressive F^- to H^- anion exchange to form $NaMgF_3$, as quick as in the second cycle.[22] After several attempts, no successful refinement of the F content was performed in the present work. Noise and interferences of the signal were observed in some experiments. On the basis of the information above, the F content in the perovskite hydride can vary accordingly with the material process history and the F

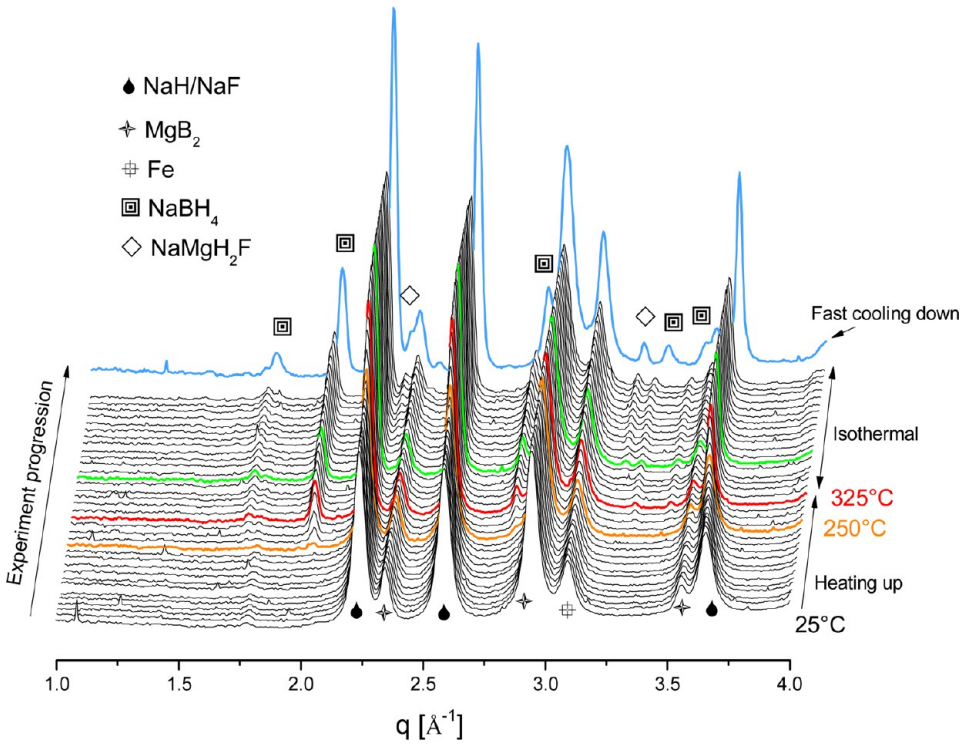

Figure 4. In situ SR-PXD hydrogenation reaction in NaF/9NaH + 5MgB_2 material at 325 °C, 25 bar hydrogen pressure, and heating rate of 5 °C min^{-1}; D3 beamline, DESY.

DOI: 10.1021/acs.jpcc.6b09776
J. Phys. Chem. C 2017, 121, 4093−4102

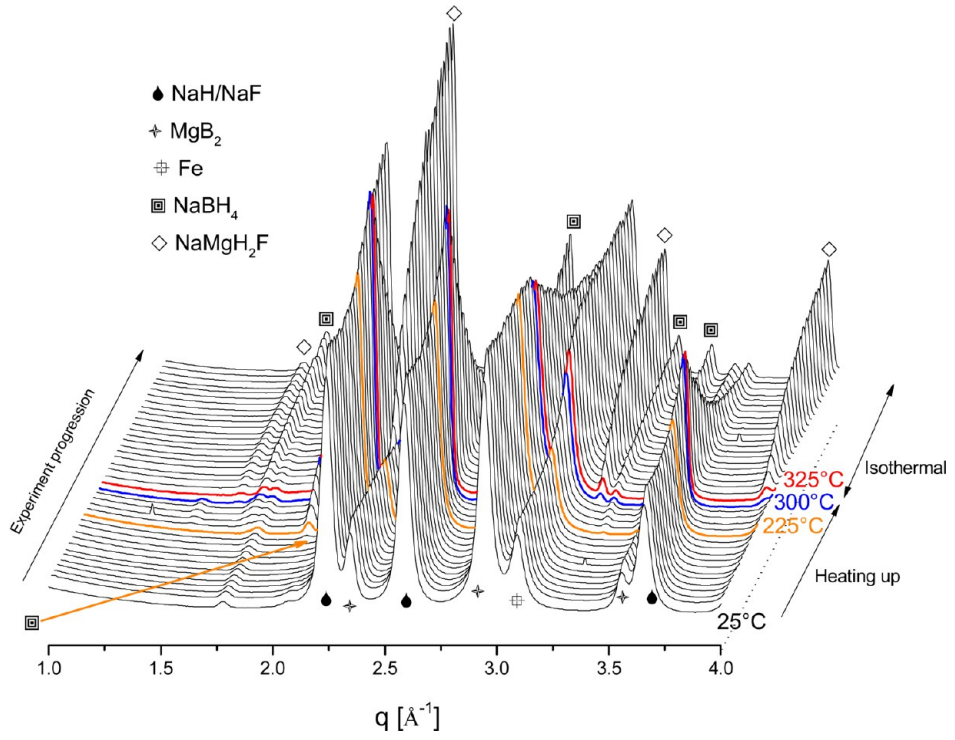

Figure 5. In situ SR-PXD hydrogenation reaction in NaF/9NaH + 5MgB_2 material at 325 °C, 50 bar hydrogen pressure, and heating rate of 5 °C min^{-1}; I711 beamline, MAX-lab.

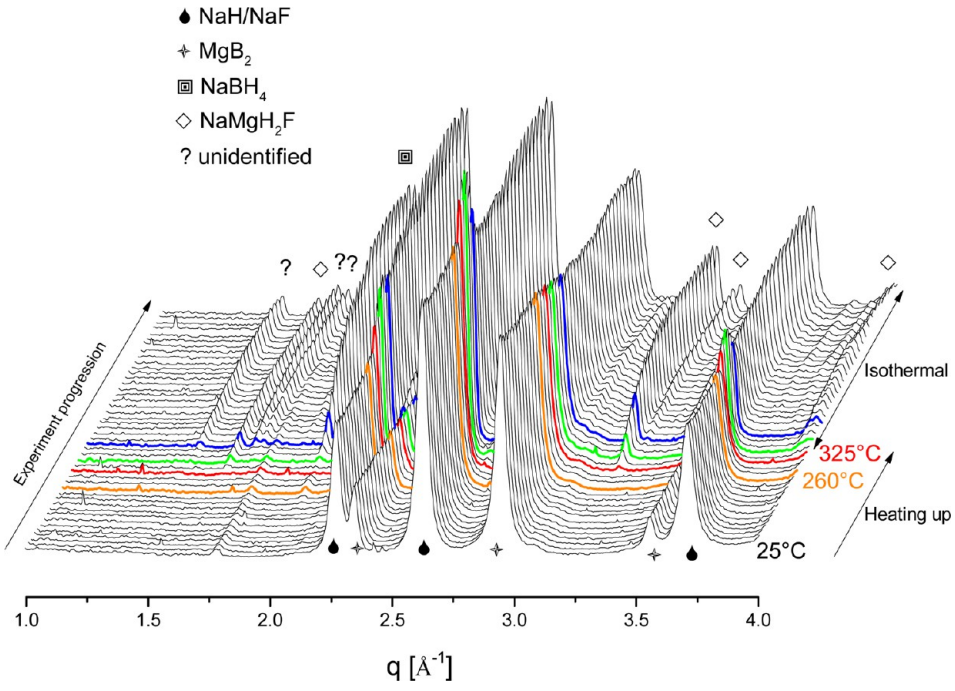

Figure 6. In situ SR-PXD hydrogenation reaction in NaF/2NaH + 1.5MgB_2 material at 325 °C, 25 bar hydrogen pressure, and heating rate of 5 °C min^{-1}; D3 beamline, DESY.

availability. And some differences on the reported dehydriding behavior of the perovskite hydride/fluoride materials can be commented: $NaMgH_3$ is a material reported to desorb hydrogen in a two-step process at 380 °C.[23,24] Meanwhile, $NaMgH_2F$ is a thermodynamically stable material that desorbs about 2.5 wt % of hydrogen above 478 °C in a single-step process and in a two-step process below 478 °C.[22] Thus, the formation of any form of the perovskite hydride/fluoride material can be considered as undesired.

Figure 5 presents the hydrogenation of NaF/9NaH + 5MgB_2 material, this time at 50 bar, traced by in situ SR-XPD. The hydrogenation reaction at 50 bar is marked by the formation of $NaBH_4$ at 225 °C (orange diffractogram) and by the formation of $NaMgH_2F$ at 300 °C (blue diffractogram). Thus, the increase

DOI: 10.1021/acs.jpcc.6b09776
J. Phys. Chem. C 2017, 121, 4093−4102

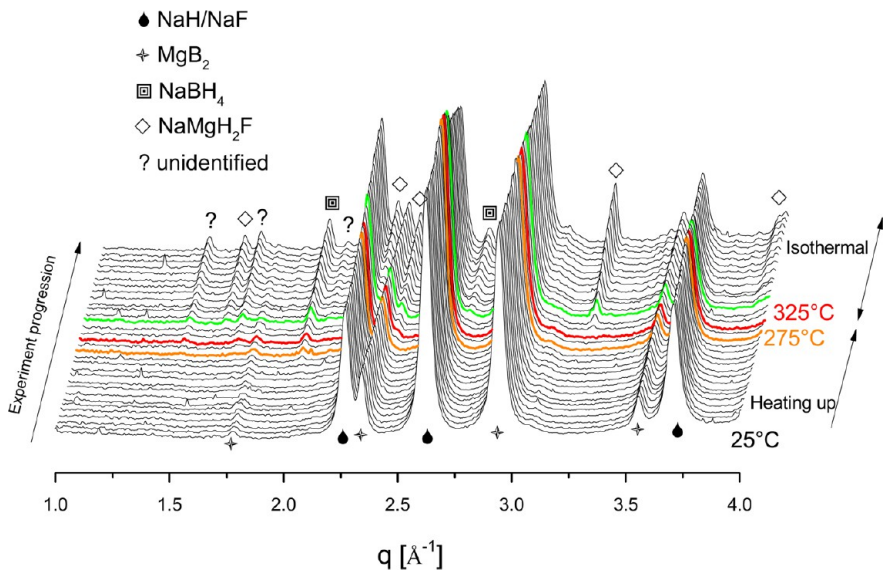

Figure 7. In situ SR-PXD hydrogenation reaction in NaF/2NaH + 1.5MgB_2 material at 325 °C, 50 bar hydrogen pressure, and heating rate of 5 °C min^{-1}; D3 beamline, DESY.

in hydrogenation pressure promoted the formation of $NaBH_4$ and $NaMgH_2F$ to a slightly lower temperature.

Figure 6 presents the in situ SR-XPD hydrogenation of the NaF/2NaH + 1.5MgB_2 at 25 bar. The hydrogenation products started growing at 260 °C with the formation of $NaBH_4$ (orange diffractogram). Shortly after reaching the isothermal condition at 325 °C, the formation of $NaMgH_2F$ became evident (green diffractogram). After this, an unidentified hydrogenation product was formed (blue diffractogram). The main peaks of this unidentified product were situated at 1.48, 1.71, 1.75, and 2.10 $Å^{-1}$. Figure 7 shows the hydrogenation of the NaF/2NaH + 1.5MgB_2 at 50 bar. The formation of $NaBH_4$ started at 275 °C, whereas the formation of $NaMgH_2F$ and an unidentified hydrogenation product with peaks at 1.46, 1.68, 1.87, 2.06, and 2.39 $Å^{-1}$, similar to Figure 6, was observed at 325 °C (green diffractogram). Regarding these unidentified peaks, a boron-rich phase (B_{48}) had been observed during hydrogenation of 2NaH/MgB_2 [25] and NaF/9NaH + 5MgB_2.[15] According to the structural data reported for that B-phase,[25] the main expected peak positions will be 1.48, 1.71, 1.91, 2.10, and 2.42 $Å^{-1}$. In the present work, some of the peaks marked as "unidentified" indeed match the expected peak positions for the B_{48}, and some not. Knowing the ability of B to form allotropes, it is highly possibly that those peaks correspond to a sort of B-cluster. Interestingly, the samples contaminated with Fe, i.e., the NaF/9NaH + 5MgB_2, did not observe the formation of the unidentified hydrogenation product with peaks close to the B_{48} phase.

3.5. Hydrogenation of NaF/NaH/MgB_2 Reactive Hydride Composites. The theoretical hydrogen storage capacity of the composites NaF/9NaH + 5MgB_2 and NaF/2NaH + 1.5MgB_2, through the formation of $NaBH_4$ and MgH_2, could be 7.6 and 7.1 wt %, respectively. Meanwhile, the nondoped 2NaH + MgB_2 composite has a theoretical hydrogen storage capacity of 7.8 wt %. Thus, a small reduction of the theoretical hydrogen capacity with the incorporation of fluorine was expected. However, the experimental hydrogen uptake was 4.8 wt % for the NaF/2NaH + 1.5MgB_2 material at 50 bar hydrogen pressure (Figure 8). The experimental hydrogen storage capacity for the rest of the materials was almost the same, between 4.2 and 4.1 wt % H_2.

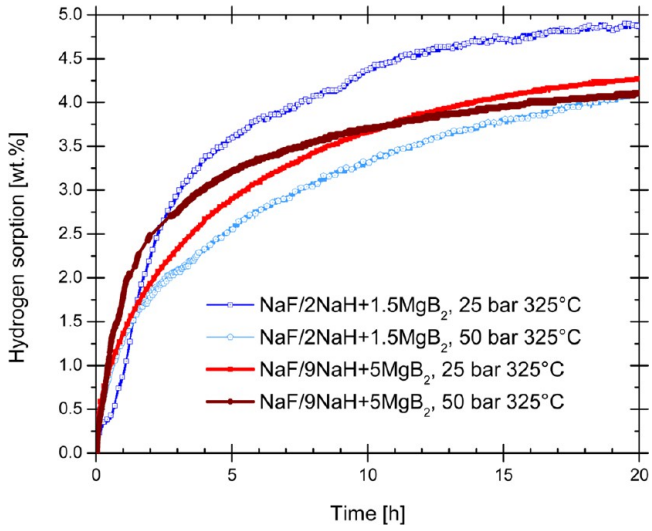

Figure 8. Hydrogenation curves of NaF/9NaH + 5MgB_2 and NaF/2NaH + 1.5MgB_2 at 325 °C and 25 and 50 bar.

PCI curves (Figure 9) demonstrate the low equilibrium pressure of the studied materials. The equilibrium pressure of NaF/9NaH + 5MgB_2 material is not so well-defined, and it was observed at about 2 bar of hydrogen pressure. Meanwhile, the equilibrium pressure of NaF/2NaH + 1.5MgB_2 was better defined at 8 bar of H_2. To the best of our knowledge, no published data on PCI for hydrogenation or dehydrogenation equilibrium pressure of 2NaH + MgB_2 or NaBH4 + MgH_2 are available. The closest reference is the (dehydrogenation) equilibrium pressure of $NaBH_4$; it was reported as 2.5 bar at 600 °C.[26] On the basis of the low hydrogenation equilibrium pressure, a lower dehydrogenation pressure (counting on dehydrogenation hysteresis) or high dehydrogenation temperature is expected. In that regard, the NaF/2NaH + 1.5MgB_2 material can be of interest due to a slightly high hydrogenation

DOI: 10.1021/acs.jpcc.6b09776
J. Phys. Chem. C 2017, 121, 4093−4102

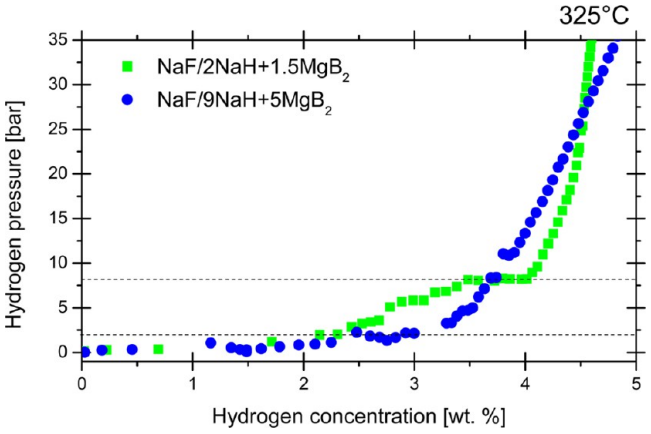

Figure 9. PCI curves of NaF/9NaH + $5MgB_2$ and NaF/2NaH + $1.5MgB_2$ at 325 °C.

equilibrium pressure that could lead to a moderate dehydrogenation pressure. This statement should be subject to research to establish appropriate dehydrogenation conditions.

3.6. Scanning Electron Microscopy of Hydrogenated Materials. Figure 10a and Figure 10b present the SEM images

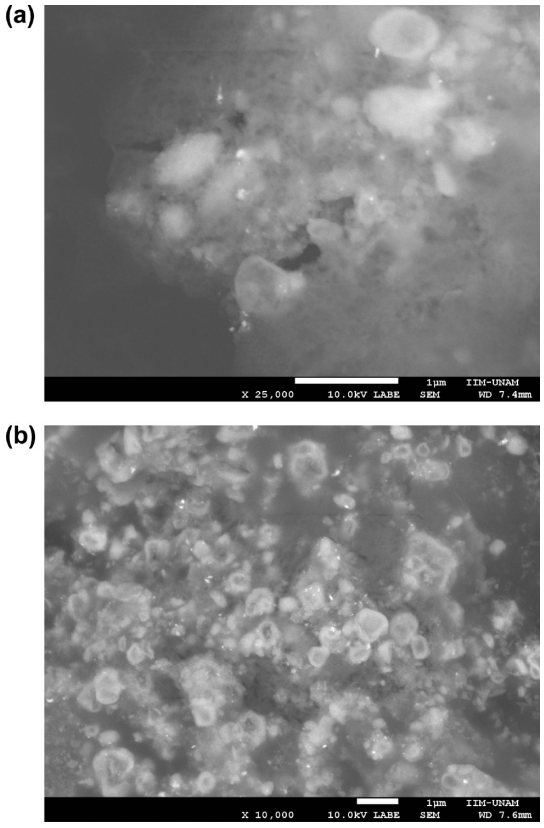

Figure 10. SEM images of (a) hydrogenated NaF/2NaH + $1.5MgB_2$ and (b) NaF/9NaH + $5MgB_2$.

of the hydrogenated NaF/2NaH + $1.5MgB_2$ and NaF/9NaH + $5MgB_2$, respectively. Both materials are heavily agglomerated. The agglomerate size was about 200−300 μm (Supporting Information). The surfaces are highly roughened, and it was difficult to identify single particles. However, quasi-spherical particles of 1 μm diameter can be distinguishable in SEM images.

3.7. Infrared Spectroscopy of Hydrogenated Materials. Anion substitution had been proposed as a way for tailoring the borohydrides properties. It had been successfully demonstrated for heavier halides such as Cl^- or Br^-, where the whole substitution of the $[BH_4]^-$ moiety is possible.[27] A bit more challenging is the substitution of H^- for F^- inside the $[BH_4]^-$ group, for both synthesis and characterization. A very important question to answer is whether or not F is substituting H in the $NaBH_4$ product. To answer this question, the most appropriate characterization technique is the FT-IR. Figure 11

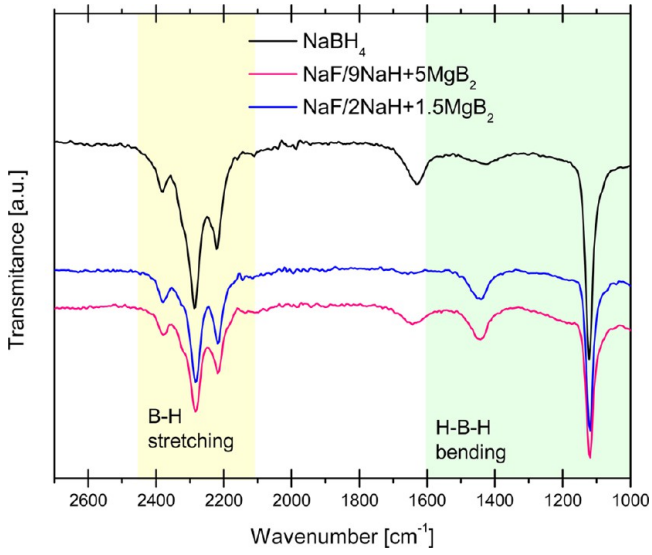

Figure 11. FT-IR spectra of hydrogenated NaF/9NaH + $5MgB_2$ and NaF/2NaH + $1.5MgB_2$ (material from PCI experiments). $NaBH_4$ (Aldrich) is for reference and visual comparison.

presents the FT-IR spectra of three materials; the hydrogenated (from PCI curve testing) NaF/9NaH + $5MgB_2$ and NaF/2NaH + $1.5MgB_2$, together with $NaBH_4$ (Aldrich) as the reference. Borohydrides present two regions of interest: the B−H bending region (1000−1500 cm^{-1}) and the H−B−H stretching region (2000−2500 cm^{-1}).[28] Peaks were observed at these regions on hydrogenated and reference materials. No peak-shifts associated with the change in vibration energy due to F to H substitution were found.

4. DISCUSSION

In brief, the main products of the hydrogenation reactions were (i) the desired $NaBH_4$ and (ii) the undesired $NaMgH_2F$. The formation of $NaBH_4$ is consistently observed at temperatures in the range of 225−275 °C and found to some degree dependent on the hydrogenation pressure. The formation of $NaMgH_2F$ was observed at 325 °C, during the isothermal period. Not all indications of MgH_2 formation were observed.

Additionally, the formation of the unidentified hydrogenation product observed at our NaF/2NaH + $1.5MgB_2$ samples, reported $2NaH/MgB_2$ [15] and reported $NaH/9NaF/5MgB_2$ [25] systems, was not observed at our NaF/9NaH + $5MgB_2$ samples. The most important difference was the presence of approximately 1.5 wt % of Fe in the NaF/9NaH + $5MgB_2$ samples. Fe is an old and well-known catalyst for hydriding/dehydriding of simple hydrides such as MgH_2. In Li-based RHC ($2LiH + MgB_2/2LiBH_4 + MgH_2$), the addition of Fe induced a reduction of the decomposition temperature by 30

DOI: 10.1021/acs.jpcc.6b09776
J. Phys. Chem. C 2017, 121, 4093−4102

°C and the formation of FeB particles.[29] Fe can act as catalyst or dopant in RHC affecting the hydrogenation mechanism and reducing the formation of these unidentified phases. Further research must be performed to clear up the role of Fe.

4.1. Effect of NaF in the Thermodynamics of the NaH/NaF/MgB_2 System. Pinatel et al.[30] calculated that the formation of a solid solution NaH−NaF has a slightly negative mixing enthalpy, i.e., less than −2 kJ mol^{-1}. These authors also indicate that the mixing enthalpy of related hydrides−fluorides such as NaH−NaF can influence the stability of the NaH.[30] However, the thermodynamic stability of both compounds is high and it changes dramatically, from the ΔH_f°(NaH) = −56.4 kJ·mol^{-1} [31] to ΔH_f°(NaF) = −573.6 kJ mol^{-1}.[32] Thus, the thermodynamic destabilization could be expected to be minor in the whole Na-RHC system.

4.2. Effect of NaF in the Kinetics and Hydrogenation Pathway of the NaH/NaF/MgB_2 System. What is well expected is a change in the kinetics and the hydrogenation pathway by the presence of NaF in the NaH/NaF/MgB_2 system. To start, let us resume the hydrogenation of NaH/MgB_2: Pistidda et al.[33,34] reported the formation of $NaBH_4$, MgH_2, and $NaMgH_3$ from the hydrogenation of a mixture of NaH and MgB_2. In these reports, the hydrogenation was carried out at 400 °C and at 50, 25, and 5 bar. The maximum hydrogen uptake was 6.2 wt % after 63 h [33] or 5.1 wt % after 21 h,[34] both at 50 bar, and 3.8 wt % at 25 bar.[33] The hydrogenation was described as a two-step reaction that proceeded by the formation of a reaction intermediary followed by the formation of $NaMgH_3$ at 330 °C and finally the formation of $NaBH_4$ at 380 °C.[33,34]

For the NaH/NaF/MgB_2 systems, the hydrogen uptake, 4.1−4.8 wt % H_2, is comparable to the undoped system. However, it is important to mention the reduction in the hydrogenation temperature and the shifted order of formation of the $NaBH_4$ and the (related) $NaMgH_2F$ presented here. As observed in the in situ SR-PXD and HP-DSC tracing, the addition of NaF to the NaH/MgB_2 affected the pathway of hydrogenation reaction.

The effects of NaF on the hydrogenation reaction pathway of NaH/MgB_2 can be summarized as follows:

(i) Decreasing of the formation temperature of $NaBH_4$. Obtained results confirmed the formation of $NaBH_4$ in the range of 225−275 °C. The formation of $NaMgH_2F$ was observed at 325 °C, i.e., during the isothermal period. Meanwhile, the formation of the MgH_2 was not evident. Heree et al. also observed the $NaBH_4$ formation at a lower temperature than $NaMgH_2F$.[15]

(ii) Undesirable formation of $NaMgH_2F$ instead of MgH_2 that has the effect of decreasing the hydrogen uptake. As stated above, $NaMgH_3$ and $NaMgH_2F$ share crystal structure. Even more, they are close regarding synthesis approaches. $NaMgH_3$ had been observed as a byproduct in 2NaH + MgB_2 hydrogenation.[6,7,33,34] $NaMgH_3$ also can be produced directly by the ball milling of NaH + MgH_2.[35] The $NaMgH_2F$ was reported as a product of the hydrogenation of a mixture of NaF + Mg 1:1 molar at 480 °C for 24 h under 10 bar of hydrogen pressure.[20] $NaMgH_2F$ is a byproduct of the hydrogenation of NaH−NaF−MgB_2 presented in this report. The thermodynamic stability of $NaMgH_2F$ makes it an undesirable hydrogenation product. On the other hand, the different temperature values observed for the formation of $NaBH_4$ and $NaMgH_2F$ could lead to selective product formation if careful control of temperature is done.

4.3. Effect of NaF Quantity in the Hydrogenation of the NaH/NaF/MgB_2 System. The effect of NaF quantity in the hydrogenation of the NaH/NaF/MgB_2 system was a change of the hydrogenation equilibrium pressure. The selection of 25 and 50 bar of hydrogenation pressure was proposed for the comparison criterion with published data on the nondoped material.[15,33,34] However, PCI curves demonstrated the exact hydrogenation equilibrium pressure values and that the hydrogenation reaction might be performed in softer conditions of pressure compared to values already reported. PCI curves also demonstrated the dependence of the RHC performance on the NaF content: the material with higher NaF content presented a more suitable hydrogenation equilibrium pressure if there was intended coupling with an H_2/O_2 polymer exchange membrane fuel cell (PEMFC).

4.4. Materials Morphology. Clear changes in the materials morphology were observed as the material story progressed. As-milled NaH−NaF presented changes accordingly with the NaF content. Increased NaF content induced a reduction in particle size. With the addition of MgB_2, a strong agglomeration and change in the particle size and morphology occurred; this is not recommended for solid−gas reactions. This might condition the hydrogen uptake, which was inferior compared to the expected.

5. CONCLUSIONS

Two Na-based RHC materials with different amount of NaF as additive, i.e., NaF/2NaH + 1.5MgB_2 and NaF/9NaH + 5MgB_2, were produced and tested for hydrogen storage at two different hydrogen pressures (25 and 50 bar). The hydrogen uptake was between 4.1 and 4.8 wt % H_2. The hydrogenation products were $NaBH_4$ and $NaMgH_2F$ plus an unidentified product probably related to B-clusters in NaF/2NaH + 1.5MgB_2 RHC. The unidentified product was absent in NaF/9NaH + 5MgB_2 RHC, material that was contaminated with 1.5 wt % Fe. The reaction pathway was demonstrated to produce first the $NaBH_4$ and then the $NaMgH_2F$, an inverted order compared to the non-NaF doped Na-RHC. The hydrogenation products, $NaBH_4$ and $NaMgH_2F$, were obtained at different temperatures, and this could make possible performance of a selective hydrogenation reaction. PCI curves demonstrated the influence of NaF content; the hydrogenation equilibrium pressures were approximately 2 and 8 bar at 325 °C for NaF/9NaH + 5MgB_2 and NaF/2NaH + 1.5MgB_2, respectively. The PCI curve of NaF/2NaH + 1.5MgB_2 RHC, i.e., the material with the higher amount of NaF, demonstrated the better definition of the equilibrium pressure plateau and a suitable value if coupling with PEMFC is intended. Morphology changed importantly starting with nanometric particles of NaF−NaH solid solutions to heavily agglomerated (micrometric) hydrogenation products.

■ ASSOCIATED CONTENT

Ⓢ Supporting Information

The Supporting Information is available free of charge on the ACS Publications website at DOI: 10.1021/acs.jpcc.6b09776.

Additional SEM images of different stages of the materials and summary of crystal information (PDF)

■ AUTHOR INFORMATION

Corresponding Author

*E-mail: karina_suarez@iim.unam.mx, karina.suarez.alcantara@gmail.com. Phone: +52 55 5623-7300, extension 37889.

DOI: 10.1021/acs.jpcc.6b09776
J. Phys. Chem. C 2017, 121, 4093−4102

ORCID

K. Suárez-Alcántara: 0000-0002-8630-2899

Present Address

[§]I.S.: Ivan Franko National University of Lviv, Kyryla and Mefodia Str. 6, 79005 Lviv, Ukraine. Participating investigator: data collection during synchrotron beam time.

Notes

The authors declare no competing financial interest.

■ ACKNOWLEDGMENTS

K.S.-A. thanks SENER-CONACyT for the funding: Project 215362 "Investigación en mezclas reactivas de hidruro: nanomateriales para almacenamiento de hidrógeno como vector energético". K.S.-A. and I.S. thank Helmholtz-Zentrum Geesthacht for the facilities and scholarship during a postdoc stay funded by The European Community in the Frame of the FP7 Project "FLYHY—Fluorine Substituted High Capacity Hydrides for Hydrogen Storage at Low Working Temperatures" (Grant 226943). K.S.-A. is very thankful to Dr. M. Dornheim and Prof. Dr. T. Klassen. Parts of this research were carried out at the light source DORIS III at DESY, a member of the Helmholtz Association (HGF). The authors thank Dr. M. Tolkiehn for assistance in using beamline D3, and Dr. U. Bösenberg during experimental SR-PXD sessions. The authors thank MAX-lab for the synchrotron facilities and technical support and particularly Dr. Dörthe Haase. HP-DSC was performed at Helmut Schmidt Universität, Institut für Werkstofftechnik, Hamburg, Germany, by Dr. M. Schulze, for which the authors are very thankful. SEM images were obtained at IIM-UNAM; the authors thank Dr. Omar Novelo and Fis. Josué Esau Romero Ibarra. The authors thank Dr. Omar Solorza Feria and CINVESTAV-Zacantenco for facilitating FT-IR characterization.

■ REFERENCES

(1) Li, H. W.; Yan, Y.; Orimo, S.; Züttel, A.; Jensen, C. M. Recent Progress in Metal Borohydrides for Hydrogen Storage. *Energies* **2011**, *4*, 185−214.

(2) Vajo, J. J.; Olson, G. L. Hydrogen Storage in Destabilized Chemical Systems. *Scr. Mater.* **2007**, *56*, 829−834.

(3) Dornheim, M.; Doppiu, S.; Barkhordarian, G.; Boesenberg, U.; Klassen, T.; Gutfleisch, O.; Bormann, R. Hydrogen Storage in Magnesium-Based Hydrides and Hydride Composites. *Scr. Mater.* **2007**, *56*, 841−846.

(4) Boesenberg, U.; Doppiu, S.; Mosegaard, L.; Barkhordarian, G.; Eigen, N.; Borgschulte, A.; Jensen, T. R.; Cerenius, Y.; Gutfleisch, O.; Klassen, T.; et al. Hydrogen Sorption Properties of MgH_2−$LiBH_4$ Composites. *Acta Mater.* **2007**, *55*, 3951−3958.

(5) Barkhordarian, G.; Jensen, T. R.; Doppiu, S.; Boesenberg, U.; Borgschulte, A.; Gremaud, R.; Cerenius, Y.; Dornheim, M.; Klassen, T.; Bormann, R. Formation of $Ca(BH_4)_2$ from Hydrogenation of CaH_2+MgB_2 Composite. *J. Phys. Chem. C* **2008**, *112*, 2743−2749.

(6) Czujko, T.; Varin, R. A.; Wronski, Z.; Zaranski, Z.; Durejko, T. Synthesis and Hydrogen Desorption Properties of Nanocomposite Magnesium Hydride with Sodium Borohydride (MgH_2 + $NaBH_4$). *J. Alloys Compd.* **2007**, *427*, 291−299.

(7) Mao, J. F.; Yu, X. B.; Guo, Z. P.; Liu, H. K.; Wu, Z.; Ni, J. Enhanced Hydrogen Storage Performances of $NaBH_4$−MgH_2 system. *J. Alloys Compd.* **2009**, *479*, 619−623.

(8) Milanese, C.; Garroni, S.; Girella, A.; Mulas, G.; Berbenni, V.; Bruni, G.; Surinach, S.; Dolores Baro, M.; Marini, A. Thermodynamic and Kinetic Investigations on Pure and Doped $NaBH_4$-MgH_2 System. *J. Phys. Chem. C* **2011**, *115*, 3151−3162.

(9) Bösenberg, U.; Kim, J. W.; Gosslar, D.; Eigen, N.; Jensen, T. R.; Bellosta von Colbe, J. M.; Zhou, Y.; Dahms, M.; Kim, D. H.; Günther, R.; et al. Role of Additives in $LiBH_4$−MgH_2 Reactive Hydride Composites for Sorption Kinetics. *Acta Mater.* **2010**, *58*, 3381−3389.

(10) Barkhordarian, G.; Klassen, T.; Bormann, R. Catalytic Mechanism of Transition-Metal Compounds on Mg Hydrogen Sorption Reaction. *J. Phys. Chem. B* **2006**, *110*, 11020−11024.

(11) Kalantzopoulos, G. N.; Guzik, M. N.; Deledda, S. R.; Heyn, H.; Muller, J.; Hauback, B. C. Destabiliztaion Effect of Transition Fluorides on Sodium Borohydride. *Phys. Chem. Chem. Phys.* **2014**, *16*, 20483−20491.

(12) Suarez-Alcantara, K.; Ramallo-Lopez, J. M.; Boesenberg, U.; Saldan, I.; Pistidda, C.; Requejo, F. G.; Jensen, T.; Cerenius, Y.; Sørby, M.; Avila, J.; et al. $3CaH_2$ + $4MgB_2$ + CaF_2 Reactive Hydride Composite as a Potential Hydrogen Storage Material: Hydrogenation and Dehydrogenation Pathway. *J. Phys. Chem. C* **2012**, *116*, 7207−7212.

(13) Saldan, I.; Ramallo-Lopez, J. M.; Requejo, F. G.; Suarez-Alcantara, K.; Bellosta von Colbe, J.; Avila, J. NEXAFS Study of 2LiF-MgB_2 Composite. *Int. J. Hydrogen Energy* **2012**, *37*, 10236−10239.

(14) Mao, J.; Guo, Z.; Liu, H.-K.; Dou, S.-X. Reversible Storage of Hydrogen in NaF-MB_2 (M=Mg, Al) Composites. *J. Mater. Chem. A* **2013**, *1*, 2806−2811.

(15) Heere, M.; Sørby, M. H.; Pistidda, C.; Dornheim, M.; Hauback, B. C. Milling Time Effect of Reactive Hydride Composites of NaF-NaH-MgB_2 Investigated by in-situ Powder Diffraction. *Int. J. Hydrogen Energy* **2016**, *41*, 13101−13108.

(16) Cerenius, Y.; Stahl, K.; Svensson, L. A.; Ursby, T.; Oskarsson, A.; Albertsson, J.; Liljas, A. The Crystallography Beamline I711 at MAX-II. *J. Synchrotron Radiat.* **2000**, *7*, 203−208.

(17) Bösenberg, U.; Pistidda, C.; Tolkiehn, M.; Busch, N.; Saldan, I.; Suarez-Alcantara, K.; Arendarska, A.; Klassen, T.; Dornheim, M. Characterization of Metal Hydrides by In-Situ XRD. *Int. J. Hydrogen Energy* **2014**, *39*, 9899−9903.

(18) Shull, C. G.; Wollan, E. O.; Morton, G. A.; Davidson, W. L. Neutron Diffraction Studies of NaH and NaD. *Phys. Rev.* **1948**, *73*, 842−847.

(19) Cortona, P. Direct Determination of Self-Consistent Total Energies and Charge Densities of Solids: A Study of the Cohesive Properties of the Alkali Halides. *Phys. Rev. B: Condens. Matter Mater. Phys.* **1992**, *46*, 2008−2014.

(20) Bouamrane, A.; Laval, J. P.; Soulie, J. P.; Bastide, J. P. Structural Characterization of $NaMgH_2F$ and $NaMgH_3$. *Mater. Res. Bull.* **2000**, *35*, 545−549.

(21) Ronnebro, E.; Noreus, D.; Kadir, K.; Reiser, A.; Bogdanovic, B. Investigation of the Perovskite Related Structures of $NaMgH_3$, $NaMgF_3$ and Na_3AlH_6. *J. Alloys Compd.* **2000**, *299*, 101−106.

(22) Sheppard, D. A.; Corgnale, C.; Hardy, B.; Motyka, T.; Zidan, R.; Paskevicius, M.; Buckley, C. E. Hydriding Characteristics of $NaMgH_2F$ with Preliminary Technical and Cost Evaluation of Magnesium-Based Metal Hydride Materials for Concentrating Solar Power Thermal Storage. *RSC Adv.* **2014**, *4*, 26552−26562.

(23) Wu, H.; Zhou, W.; Udovic, T. J.; Rush, J. J.; Yildirim, T. Crystal Chemistry of Perovskite-Type Hydride $NaMgH_3$: Implications for Hydrogen Storage. *Chem. Mater.* **2008**, *20*, 2335−2342.

(24) Ikeda, K.; Kato, S.; Shinzato, Y.; Okuda, N.; Nakamori, Y.; Kitano, A.; Yukawa, H.; Morinaga, M.; Orimo, S. Thermodynamical Stability and Electronic Structure of a Perovskite-Type Hydride, $NaMgH_3$. *J. Alloys Compd.* **2007**, *446*−*447*, 162−165.

(25) Pistidda, C.; Napolitano, E.; Pottmaier, D.; Dornheim, M.; Klassen, T.; Baricco, M.; Enzo, S. Structural Study of a New B-rich Phase Obtained by Partial Hydrogenation of 2NaH+MgB_2. *Int. J. Hydrogen Energy* **2013**, *38*, 10479−10484.

(26) Martelli, P.; Caputo, R.; Remhof, A.; Mauron, P.; Borgschulte, A.; Zuttel, A. Stability and Decomposition of $NaBH_4$. *J. Phys. Chem. C* **2010**, *114*, 7173−7177.

(27) Rude, L. H.; Nielsen, T. K.; Ravnsbæk, D. B.; Bösenberg, U.; Ley, M. B.; Richter, B.; Arnbjerg, L. M.; Dornheim, M.; Filinchuk, Y.; Besenbacher, F.; et al. Tailoring Properties of Borohydrides for Hydrogen Storage: A Review. *Phys. Status Solidi A* **2011**, *208* (8), 1754−1773.

DOI: 10.1021/acs.jpcc.6b09776
J. Phys. Chem. C 2017, 121, 4093−4102

(28) D'Anna, V.; Spyratou, A.; Sharma, M.; Hagemann, H. FT-IR Spectra of Inorganic Borohydrides. *Spectrochim. Acta, Part A* **2014**, *128*, 902−906.
(29) Puszkiel, J. A.; Gennari, F. C.; Arneodo Larochette, P.; Ramallo-Lopez, J. M.; Vainio, U.; Karimi, F.; Pranzas, P. K.; Troiani, H.; Pistidda, C.; Jepsen, J.; et al. Effect of Fe Additive on the Hydrogenation-Dehydrogenation Properties of $2LiH+MgB_2$/$2LiBH_4+MgH_2$ System. *J. Power Sources* **2015**, *284*, 606−616.
(30) Pinatel, E. R.; Corno, M.; Ugliengo, P.; Baricco, B. Effects of Metastability on Hydrogen Sorption in Fluorine Substituted Hydrides. *J. Alloys Compd.* **2014**, *615*, S706−S710.
(31) Zumdahl, S. S. *Chemical Principles*, 6th ed.; Houghton Mifflin Company, 2009.
(32) Chartrand, P.; Pelton, A. D. Thermodynamic Evaluation and Optimization of the LiF-NaF-KF-MgF_2-CaF_2 System Using the Modified Quasi-Chemical Model. *Metall. Mater. Trans. A* **2001**, *32*, 1385−1396.
(33) Pistidda, C.; Garroni, S.; Bonatto-Minella, C.; Dolci, F.; Jensen, T. R.; Nolis, P.; Bosenberg, U.; Cerenius, Y.; Lohstroh, W.; Fichtner, M.; Dolores-Baro, M.; et al. Pressure Effect on the 2NaH + MgB_2 Hydrogen Absorption Reaction. *J. Phys. Chem. C* **2010**, *114*, 21816−21823.
(34) Pistidda, C.; Pottmaier, D.; Karimi, F.; Garroni, S.; Rzeszutek, A.; Tolkiehn, M.; Fichtner, M.; Lohstroh, W.; Baricco, M.; Klassen, T.; et al. Effect of NaH/MgB_2 Ratio on the Hydrogen Absorption Kinetics of the System NaH + MgB_2. *Int. J. Hydrogen Energy* **2014**, *39*, 5030−5036.
(35) Komiya, K.; Morisaku, N.; Rong, R.; Takahashi, Y.; Shinzato, Y.; Yukawa, H.; Morinaga, M. Synthesis and Decomposition of Perovskite-Type Hydrides, $MMgH_3$ (M = Na, K, Rb). *J. Alloys Compd.* **2008**, *453*, 157−160.

DOI: 10.1021/acs.jpcc.6b09776
J. Phys. Chem. C 2017, 121, 4093−4102